doi:10.1093/brain/aww198 BRAIN 2016: 139; 2679–2693 | 2679

BRAIN
A JOURNAL OF NEUROLOGY

# Widespread changes in network activity allow non-invasive detection of mesial temporal lobe seizures

**Alice D. Lam, Rodrigo Zepeda, Andrew J. Cole and Sydney S. Cash**

Decades of experience with intracranial recordings in patients with epilepsy have demonstrated that seizures can occur in deep cortical regions such as the mesial temporal lobes without showing any obvious signs of seizure activity on scalp electroencephalogram. Predicated on the idea that these seizures are purely focal, currently, the only way to detect these 'scalp-negative seizures' is with intracranial recordings. However, intracranial recordings are only rarely performed in patients with epilepsy, and are almost never performed outside of the context of epilepsy. As such, little is known about scalp-negative seizures and their role in the natural history of epilepsy, their effect on cognitive function, and their association with other neurological diseases. Here, we developed a novel approach to non-invasively identify scalp-negative seizures arising from the mesial temporal lobe based on scalp electroencephalogram network connectivity measures. We identified 25 scalp-negative mesial temporal lobe seizures in 10 patients and obtained control records from an additional 13 patients, all of whom underwent recordings with foramen ovale electrodes and scalp electroencephalogram. Scalp data from these records were used to train a scalp-negative seizure detector, which consisted of a pair of logistic regression classifiers that used scalp electroencephalogram coherence properties as input features. On cross-validation performance, this detector correctly identified scalp-negative seizures in 40% of patients, and correctly identified the side of seizure onset for each seizure detected. In comparison, routine clinical interpretation of these scalp electroencephalograms failed to identify any of the scalp-negative seizures. Among the patients in whom the detector raised seizure alarms, 80% had scalp-negative mesial temporal lobe seizures. The detector had a false alarm rate of only 0.31 per day and a positive predictive value of 75%. Of the 13 control patients, false seizure alarms were raised in only one patient. The fact that our detector specifically recognizes focal mesial temporal lobe seizures based on scalp electroencephalogram coherence features, lends weight to the hypothesis that even focal seizures are a network phenomenon that involve widespread neural connectivity. Our scalp-negative seizure detector has clear clinical utility in patients with temporal lobe epilepsy, and its potential easily translates to other neurological disorders, such as Alzheimer's disease, in which occult mesial temporal lobe seizures are suspected to play a significant role. Importantly, our work establishes a novel approach of using computational approaches to non-invasively detect deep seizure activity, without the need for invasive intracranial recordings.

Department of Neurology, Massachusetts General Hospital, Boston, MA 02114, USA

Correspondence to: Alice D. Lam, MD PhD,
Department of Neurology, Massachusetts General Hospital,
WACC 735, 55 Fruit Street, Boston, MA 02114
USA
E-mail: adlam@partners.org

**Keywords:** temporal lobe epilepsy; temporal lobe; intracranial EEG; Alzheimer's disease; seizure detection

**Abbreviation:** PCA = principal component analysis

Received February 12, 2016. Revised May 12, 2016. Accepted June 20, 2016. Advance Access publication July 29, 2016

# Introduction

Temporal lobe epilepsy is the most common human focal epilepsy (Engel, 2001). The mesial temporal lobe is one of the most epileptogenic regions of the brain, yet it is also one of the most difficult regions to record from on scalp EEG. Studies using combined recordings of intracranial electrodes and scalp EEG have demonstrated that 25% of patients with medication-refractory temporal lobe epilepsy have entire seizures recorded on intracranial electrodes that show no clear ictal correlate on scalp EEG (Ebersole and Pacia, 1996; Pacia and Ebersole, 1997). These seizures are generally considered to involve only deep mesial structures. Mesial temporal lobe seizures that lack a scalp ictal correlate are often electrographic seizures that occur without obvious clinical manifestations. An intracranial depth electrode study in patients with temporal lobe epilepsy showed that 80% of seizures that arose focally and that remained focal within the mesial temporal lobe were not associated with any clinical symptoms (Wennberg *et al.*, 2002). Another study using intracranial electrodes found that 90% of subclinical temporal lobe seizures and 82% of auras had no demonstrable ictal changes on scalp EEG (Lieb *et al.*, 1976).

Without obvious accompanying clinical symptoms or scalp EEG findings to identify these mesial temporal lobe seizures, clinicians are essentially blind to the existence of these seizures without the aid of intracranial recordings. Yet, only a minority of patients will ever undergo invasive intracranial recordings, given the risks and costs involved. Better and non-invasive tools are needed to detect these 'scalp-negative' seizures. Such a tool would be useful not only for diagnosis and subsequent management of these seizures, but could yield a better understanding of the clinical significance of these seizures in temporal lobe epilepsy. Furthermore, there may be specific neurological conditions, such as the dementias, in which these otherwise undetectable seizures may play a key pathophysiologic role (Sanchez *et al.*, 2012; Scharfman, 2012; Vossel *et al.*, 2013; Horvath *et al.*, 2016).

To date, the lack of a scalp EEG ictal correlate in a subset of temporal lobe seizures has been described based on visual analysis of scalp EEG recordings. These seizures often show non-specific changes on scalp EEG, such as interruption of background activity or irregular slowing (Ebersole and Pacia, 1996; Pacia and Ebersole, 1997). Quantitative analysis of EEG recordings can yield important details regarding the spatial, spectral, temporal, and network properties of cortical activity that may not otherwise be discernible on visual inspection of the EEG (Bartolomei *et al.*, 1999; Zaveri *et al.*, 2001). We hypothesized that the changes on scalp EEG during scalp-negative mesial temporal lobe seizures would have a distinct quantitative scalp EEG signature, which could be used to identify these seizures on scalp EEG alone, without the need for invasive intracranial recordings. Given the emerging hypothesis that even focal seizures may involve widespread neural networks (Kramer and Cash, 2012; Laufs, 2012), we were interested in determining whether a scalp EEG functional connectivity signature could be used to detect these focal mesial temporal lobe seizures.

Here, we demonstrate a novel approach to non-invasively study scalp-negative mesial temporal lobe seizures in humans, without the need for invasive intracranial electrodes. We used a training dataset of scalp-negative mesial temporal lobe seizures that were identified in patients with temporal lobe epilepsy who underwent simultaneous recordings with foramen ovale electrodes and scalp EEG. We then tuned logistic regression classifiers to detect these seizures based on scalp EEG coherence properties. On cross-validation, our detector correctly identified scalp-negative mesial temporal lobe seizures in 40% of patients—a notable advance, considering that on routine clinical interpretation of these scalp EEGs, none of these patients are found to have scalp-negative seizures. Moreover, our detector correctly identified the side of seizure onset in all seizures that were detected. Our detector was highly specific, with a false alarm rate of only 0.31 per day and a positive predictive value of 75%. Eighty per cent of patients in whom detections were made actually had scalp-negative mesial temporal lobe seizures. The ability of our detector to specifically recognize focal mesial temporal lobe seizures based on scalp EEG coherence properties provides support for the hypothesis that even focal seizures involve widespread neural networks. Importantly, our approach provides the first opportunity to study scalp-negative seizures in a wide population of patients and paves the way to understanding the role of scalp-negative mesial temporal lobe seizures in patients with epilepsy and related neurological and psychiatric disorders.

# Materials and methods

## Patient population

Data were obtained from patients who underwent monitoring with simultaneous foramen ovale electrodes and scalp EEG electrodes at our institution from 2009 to 2015. Analysis of these data was performed retrospectively under a protocol monitored by the Institutional Review Board at our centre. Only patients with temporal lobe epilepsy based on electrophysiological and structural studies were included for analysis. Patients in whom localization of seizure onsets remained unclear were excluded from analysis. Patients who had previously undergone brain surgery (e.g. partial anterior temporal lobectomy, tumour resection, or shunt placement) or who had extra-temporal structural brain anomalies (e.g. cortical tubers) were also excluded from analysis.

## EEG and foramen ovale electrode recordings

Foramen ovale electrodes were four-contact electrodes (Ad-Tech) that were placed bilaterally under fluoroscopic guidance

through the foramen ovale to lie in the ambient cistern, adjacent to the mesial temporal lobe (Wieser *et al.*, 1985; Sheth *et al.*, 2014). We used data from foramen ovale electrodes (rather than from depth electrodes) in our analysis, as foramen ovale electrodes enter the cranium through naturally occurring holes in the skull and thus do not introduce a new skull defect, which might alter the properties of the scalp EEG compared to a normal, intact skull. Scalp electrodes were placed using the International 10–20 configuration with additional anterior temporal electrodes (T1, T2). Scalp EEG and foramen ovale electrode recordings were captured using XLTEK hardware (Natus Medical Inc), with data sampled at 256, 512, or 1024 Hz.

## Identification of scalp-negative seizures

Scalp-negative seizures were initially identified by reviewing the clinical EEG reports from patients meeting our inclusion/exclusion criteria above. Seizures that were reported as showing no change on scalp EEG or no scalp ictal correlate were visually analysed independently by two board-certified clinical neurophysiologists (A.D.L., R.Z.). The neurophysiologists were allowed to review the scalp EEG data (standard 10–20 configuration with T1/T2 electrodes) as they typically would for routine clinical purposes. All EEG data were recorded referentially and could be reformatted into any montage the reviewers preferred, including (but not limited to) anterior-posterior bipolar montage with coronal ring, common and average referential montages. Reviewers could easily switch between montages during their review. Seizures were classified as scalp-negative seizures if both neurophysiologists were unable to identify a scalp ictal correlate for the seizure. Scalp-negative seizures could show subtle changes in background on scalp EEG (e.g. irregular slowing, fast activity, or even isolated sharp waves), as long as this activity was not clearly rhythmic or evolving. Scalp-negative seizure records that were compromised by excessive myogenic or electrode artefacts based on the judgement of the clinical neurophysiologists were excluded from analysis. The neurophysiologists also marked the exact start time and duration of the scalp-negative seizures based on the ictal foramen ovale electrode recordings. On foramen ovale electrodes, scalp-negative seizures were identified as $\geqslant 3$ Hz rhythmic spiking activity with evolution in frequency and voltage, lasting at least 10 s. A typical scalp-negative seizure is shown in Fig. 1.

## Seizure records

Seizure records were comprised of scalp EEG recordings of a scalp-negative seizure with up to 3 h before and 3 h after the seizure (up to 6 h total). Only one scalp-negative seizure per record was used for analysis; if other seizures occurred within the record, these were marked for exclusion from analysis in that record. Control records consisted of 6 h of seizure-free scalp EEG recording and were obtained from patients who underwent scalp EEG and foramen ovale electrode recordings but who did not contribute seizure records to the data (e.g. they either did not have scalp-negative seizures or their data had been excluded from analysis based on criteria described above). Control records were chosen to fall within the first 48 h of foramen ovale electrode implantation and to span both awake and asleep states for each patient. An additional *post hoc* control used scalp-positive seizure records from the control patients for whom these data were available. These records were similar to scalp-negative seizure records but contained a scalp-positive seizure with up to 3 h before and after the seizure (up to 6 h total).

## Coherence analysis

For coherence analysis, raw, unfiltered scalp EEG data were used to minimize phase distortion. Records were visually analysed for quality control, and sections of the record containing large-amplitude artefacts or bad channels were marked for exclusion from analysis. All subsequent analysis was performed in MATLAB (Mathworks, Natick, MA), using a combination of custom scripts and freely available scripts, including EEGLab (Delorme and Makeig, 2004) and the Chronux toolbox (Mitra and Bokil, 2008). Scalp EEGs (standard 10–20 electrodes with additional T1/T2 electrodes) were formatted into an anterior-posterior (AP) bipolar montage with a coronal ring (T1-T3, T3-C3, C3-Cz, Cz-C4, C4-T4, T4-T2, T1-T2), resulting in 25 bipolar scalp EEG channels. Each bipolar channel was normalized to zero-mean, unit variance. Multi-taper coherograms were created using the Chronux script *cohgramc* with the following parameters: frequency range analysed: 1–50 Hz, window: 2 s, step size: 1 s, time-bandwidth product: 2, tapers: 3. This yielded a spectral resolution of 2 Hz. The coherence for each channel was then averaged into five frequency bands: delta (1–4 Hz), theta (4–8 Hz), alpha (8–12 Hz), beta (12–30 Hz), and gamma (30–50 Hz). This resulted in 1500 channel-channel-frequency combinations of coherence data (300 unique channel-channel combinations $\times$ five frequency bands) for each 2-s window.

## Feature extraction

Feature vectors for seizure classification were based on scalp EEG coherence (Fig. 2). We used 2-s test epochs as this provided a balance between adequate spectral resolution and the ability to sample dynamic changes that might occur during a seizure. For each 2-s test epoch, coherence features consisted of the change in coherence of the 2-s test segment with respect to its preceding 2-min baseline segment (with a 1-min buffer segment separating the baseline and test segments). Specifically, coherence features for each epoch were calculated as the difference between the test segment median coherence and the baseline median coherence, divided by the baseline median coherence, for each channel-channel-frequency combination. Feature vectors for all test epochs within each seizure record were calculated with a 1-s step size between consecutive epochs. Test epochs were excluded from analysis if: (i) the 2-s test segment contained any large amplitude artefacts; or (ii) $>10\%$ of the 2-min baseline segment consisted of large amplitude artefacts. Each feature for each data record was standardized to zero-mean, unit variance prior to analysis. All features that involved bad electrodes were set to 0 (e.g. no change from baseline).

An additional set of feature vectors was created by transforming the coherence feature vectors as generated above to their principal component scores. Principal component analysis (PCA) was performed using all coherence feature vectors,

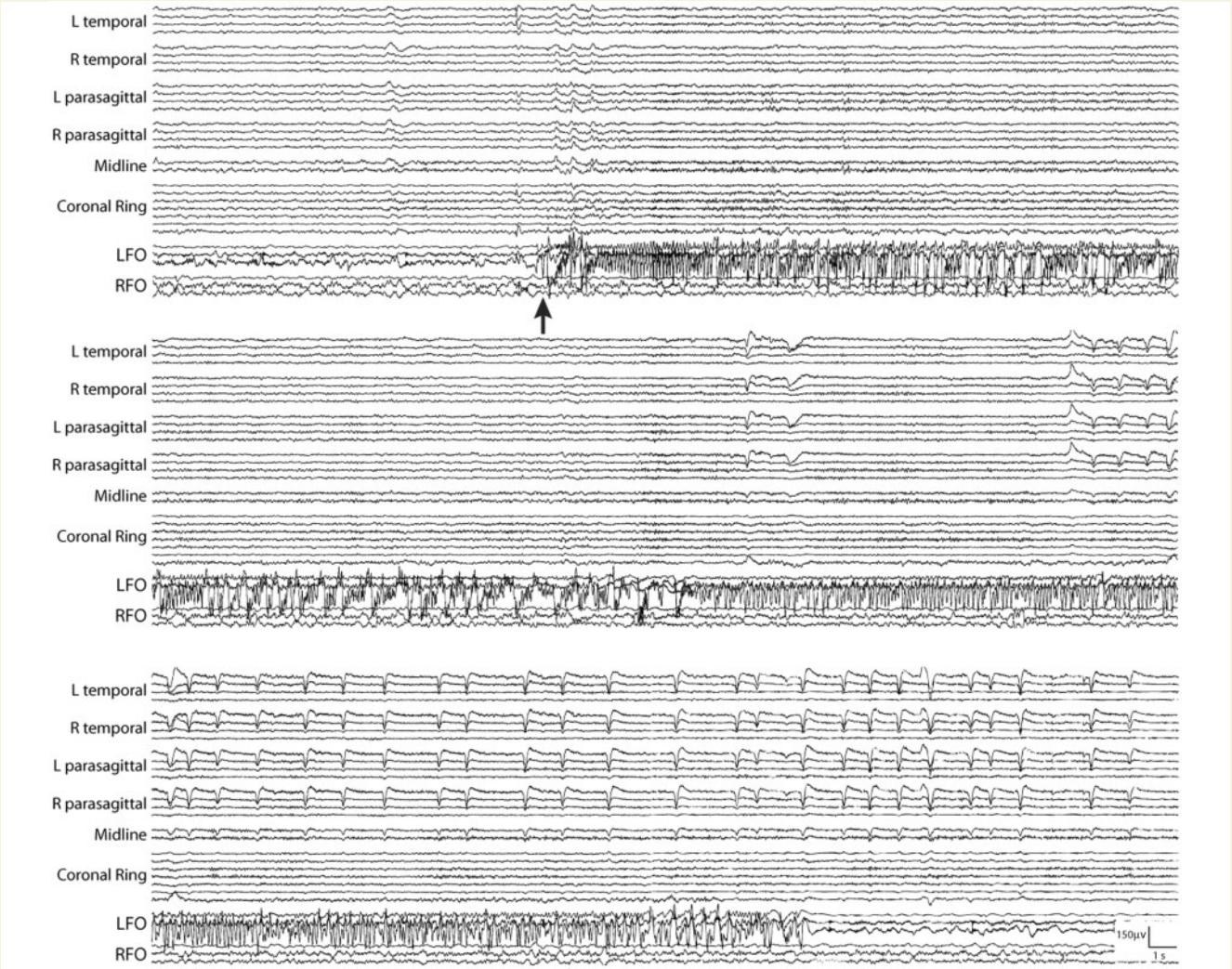


**Figure 1 Representative EEG of a scalp-negative seizure.** The seizure starts focally in the left foramen ovale electrodes (arrow) and lasts 80 s, without a clear scalp EEG ictal correlate during this time. Scalp EEG is displayed as an anterior-posterior bipolar montage with coronal ring, and the chains are arranged from top to bottom as: left temporal chain (Fp1-F7, F7-T3, T3-T5, T5-O1), right temporal chain (Fp2-F8, F8-T4, T4-T6, T6-O2), left parasagittal chain (Fp1-F3, F3-C3, C3-P3, P3-O1), right parasagittal chain (Fp2-F4, F4-C4, C4-P4, P4-O2), midline chain (Fz-Cz, Cz-Pz), and coronal ring (T1-T3, T3-C3, C3-Cz, Cz-C4, C4-T4, T4-T2, T2-T1). Shown below the scalp EEG channels are the foramen ovale electrodes (LFO = left foramen ovale; RFO = right foramen ovale) in a unilateral bipolar montage (LFO1-LFO2, LFO2-LFO3, LFO3-LFO4; and RFO1-RFO2, RFO2-RFO3, RFO3-RFO4), where contact 1 is the deepest foramen ovale electrode contact. A calibration bar is shown in the *bottom right* of the figure. The three panels represent consecutive pages of EEG recording.

for all seizure and control records combined. The same linear transformation was then applied to all coherence features to generate the principal component scores.

## Seizure detection

### Classifiers

Logistic regression was implemented using the *glmfit* function in the MATLAB machine learning toolbox (Mathworks, Natick, MA), and was used to classify feature vectors from each test epoch as belonging to either the seizure (positive) class or non-seizure (negative) class. Within each seizure record, a seizure alarm was raised whenever any 4 of 10 consecutive test epochs were classified as belonging to the seizure class (Fig. 3B). Seizure detection rates and false alarm rates were then calculated. Clusters that overlapped with any portion of the scalp-negative seizure or that fell within 60 s of the start or end of the seizure were labelled as true seizure detections; otherwise they were labelled as false alarms.

## Thresholding detection

The raw output of a logistic regression classifier is a probability between 0 and 1, and a threshold must be set to distinguish positive from negative class detections. Tuning this threshold determines the trade-off between sensitivity and specificity of classification. For each round of logistic regression training

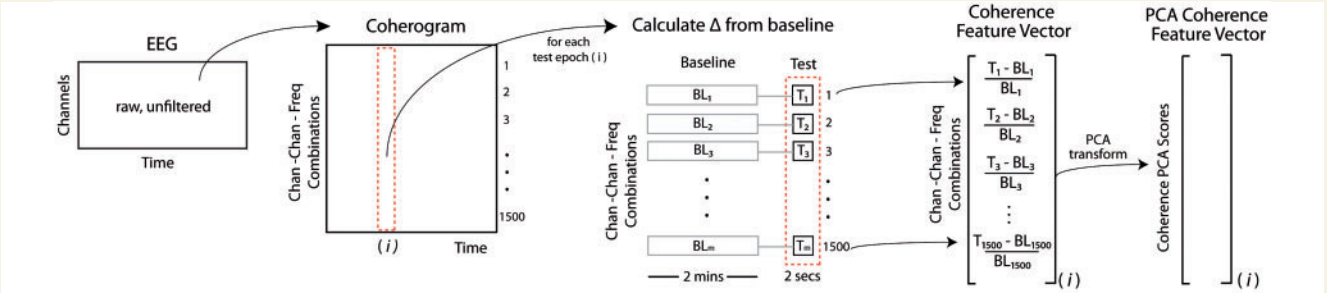


**Figure 2 Schematic illustrating determination of coherence and coherence PCA feature vectors.** Note that a feature vector is created for each 2-s test epoch within seizure and control records, with a 1-s step size between consecutive test epochs.

as described below, we chose the threshold that maximized the number of seizure detections in the training set, while limiting the training false alarm rate to $<0.08$ false alarms per hour ($\sim$2 per day). This optimized threshold was then used for cross-validation.

### Leave-one-patient-out cross-validation overview

Testing of the seizure detector used a 'leave-one-patient-out' cross-validation approach, which estimates how well the detector's performance generalizes to new patients. This was particularly important for our scalp-negative seizure detector, which we designed for use as a patient independent detector. For a total of $n$ patients, the detector was trained on all seizure records from $(n-1)$ patients and then tested on records from the remaining one patient. This procedure was repeated $n$ times, such that each patient's records were tested on separately. The overall cross-validation performance was then calculated by averaging the performance metrics (e.g. seizure detection rate, false alarm rate, etc.) across all patients.

To maximize the detector's ability to identify scalp EEG signatures associated with scalp-negative mesial temporal lobe seizures, we first trained the detector to detect only left-sided scalp-negative seizures. Our reasoning was that left-sided scalp-negative seizures would be associated with scalp EEG changes primarily over the left hemisphere, whereas right-sided scalp-negative seizures would show changes primarily over the right hemisphere. Training the detector on both types of seizures (two different signals) would reduce the detector's ability to discriminate between seizure and non-seizures states. We also reasoned that the scalp EEG signatures of left- and right-sided scalp-negative seizures would be mirror images of each other, and thus, a left-sided scalp-negative seizure detector could also be used to detect right-sided scalp-negative seizures, by providing the detector with a mirror image (left-right 'flip') of the scalp EEG data.

As such, prior to training the detector, we performed a left-right flip (reflection) of all seizure records with right-sided seizure onsets, so that all seizures for training appeared to arise from the left (Fig. 3A). During cross-validation (and in 'real life' application), however, the side of seizure onset (if a seizure occurs) is not known *a priori*. Therefore, during cross-validation, we applied the seizure detector to both the original seizure record, as well as to a left-right flipped version of the seizure record, so that both left- and right-sided scalp-negative seizures could be detected, respectively (Fig. 3B).

Left and right-sided detections were then combined. Any detections that fell within 60 s of one another were merged into a single detection that spanned both original detections. Any detection that was captured in both left and right-sided detections was discarded, with the reasoning that symmetric changes on scalp EEG are unlikely to be caused by focal seizures.

## Automated backwards feature selection

We used an automated backwards feature selection algorithm to reduce feature sets to only those features most important for seizure detection. In this algorithm, logistic regression (using the leave-one-patient-out cross-validation approach) was first applied using all 1500 coherence features. The features were then ranked by importance, based on the mean $P$-values of their regression coefficients across all patients. Features with $P$-values $>0.05$ were discarded, with a maximum of 5% of the feature set being discarded in any one iteration of the algorithm. If all features in a particular iteration had $P$-values $<0.05$, the algorithm discarded the two features with the highest $P$-values. After discarding features, a new iteration of logistic regression was performed on the reduced feature set, and further features were discarded. Iterations of the algorithm continued until there were less than five features remaining. The best feature set was chosen as the iteration with the highest average seizure detection rate per patient on cross validation. If multiple iterations were tied for the highest seizure detection rate, the iteration with the lowest cross-validation false alarm rate was chosen.

## Detector voting

To improve the specificity of detection, we applied a two detector voting system (Fig. 3C). A detection was considered 'real' only if it was captured on both the detector based on the coherence features and the detector based on the coherence PCA features. All other detections were discarded.

# Results

## Patient demographics

From 2009 to 2015, 47 patients underwent phase II presurgical evaluation with simultaneous foramen ovale

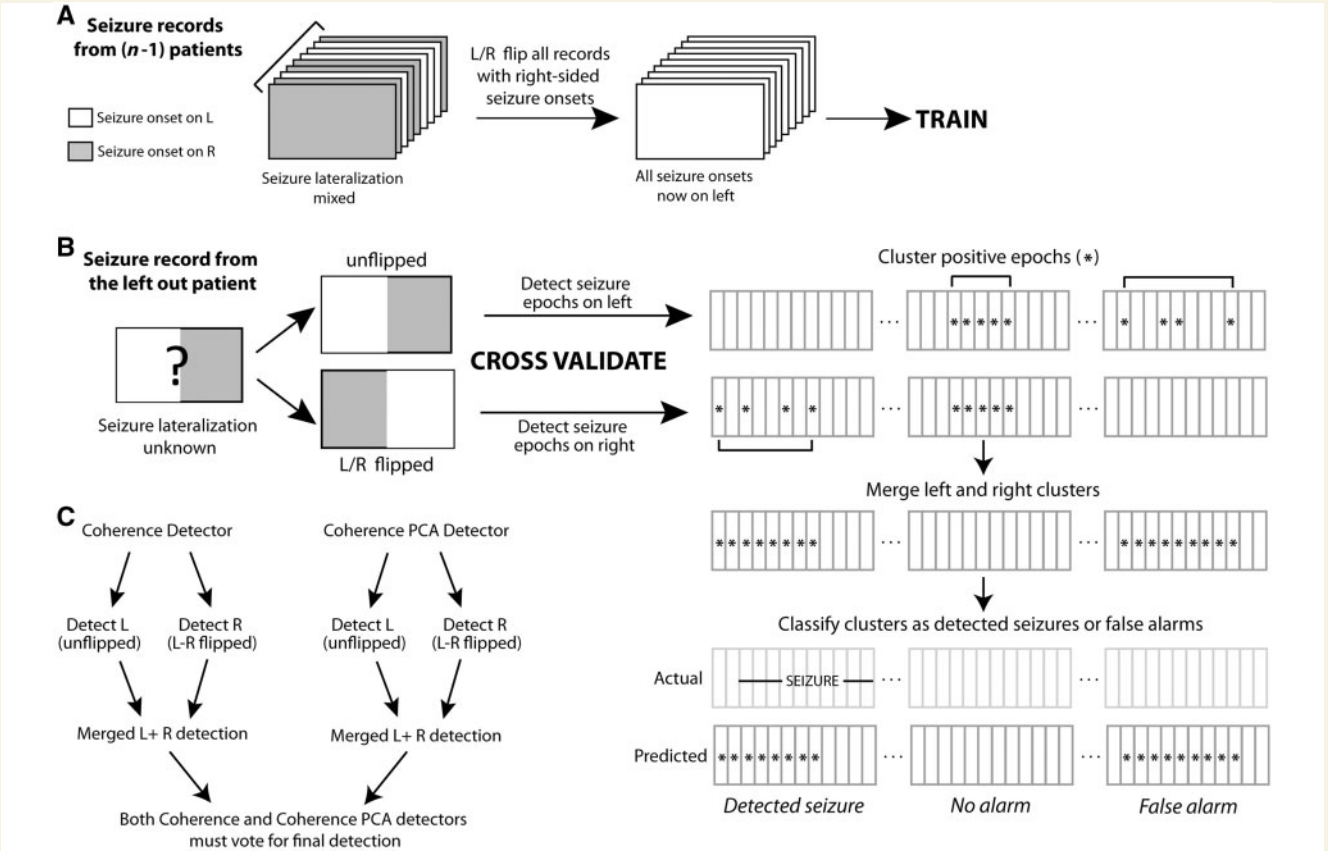


**Figure 3 Schematic illustrating approach to seizure detection with leave-one-patient-out cross-validation.** (**A**) Each round of training uses all seizure records from all but one patient, leaving the seizure records of the remaining patient for cross-validation. Seizures for training with right-sided onset are left-right flipped so that all seizure onsets appear on the left. The logistic regression classifier is thus trained to detect left-sided scalp-negative seizures. (**B**) After each round of training, the detector is tested on the seizure records from the left-out patient. Because the lateralization of the test seizure is not known *a priori*, the detector is tested on both the original seizure record (to detect left-sided seizures) as well as a left-right flipped version of the seizure record (to detect right-sided seizures). All positive epochs from each detection are then clustered, whereby at least 4 of 10 consecutive epochs must be positive to generate a cluster. Detected clusters are then merged for the left and right-sided detectors, and the final clusters are classified as either true seizure detections or false alarms. (**C**) Overview of the scalp-negative seizure combined detection scheme. Detections must be captured on both coherence and coherence PCA detectors to be considered valid.

electrode and scalp EEG recordings. We excluded 19 patients from our study due to: (i) missing EEG files or inadequate information in clinical EEG reports to determine whether/when scalp-negative mesial temporal lobe seizures occurred (seven patients); (ii) presence of intracranial anatomical abnormalities (four patients); (iii) suspected extra-temporal seizure onset (three patients); or (iv) no seizures captured (five patients). Of the remaining 28 patients with temporal lobe epilepsy, 14 had at least one scalp-negative seizure, of which 10 patients contributed seizure records to our analysis. Eleven scalp-negative seizures from six patients were excluded from analysis due to compromised quality of the EEG recordings [i.e. excessive artefact (five seizures), or excessive ictal/interictal activity at baseline (six seizures)]. A total of 25 scalp-negative seizure records from 10 patients were used in our study. An additional 13 control records (containing no seizures) were taken from 13 patients who did not contribute scalp-negative seizure records to the analysis. Combining scalp-negative seizure records and control non-seizure records, a total of 189 h of EEG data were analysed.

Table 1 shows demographic information for the patients who contributed seizure or control records to the study. Of the 10 patients with at least one scalp-negative seizure, nine had additional seizures captured that were visible on scalp EEG, whereas one patient had scalp-negative seizures as their only seizure type. The median scalp-negative seizure duration was 36 s, with seizures ranging from 13 to 110 s in duration. Nineteen of the 25 scalp-negative seizures had onset in the left foramen ovale electrodes, whereas six had onset in the right foramen ovale electrodes.

## Semiology of scalp-negative seizures

Clinical manifestations of scalp-negative seizures were analysed using descriptions from clinical EEG reports.

**Table 1 Patient demographics**

| Patient | Age (y) | Sex | Scalp negative seizures, *n* | Other seizures visible on scalp? | Seizure onset lateralization | Surgery | Surgical pathology | Outcome |
|---|---|---|---|---|---|---|---|---|
| 1 | 26 | F | 4 | Yes | Left | Left ATL | Hippocampal sclerosis | Seizure-free at 4 years |
| 2 | 42 | F | 1 | Yes | Left | | | |
| 3 | 46 | M | 3 | Yes | Right | Right ATL | Hippocampal sclerosis | Seizure-free at 3 years |
| 4 | 33 | F | 3 | Yes | Left | Left ATL | Hippocampal sclerosis | Seizure-free at 2 years |
| 5 | 33 | M | 1 | Yes | Left | Left ATL | Subependymal gliosis | Seizure-free at 5 years |
| 6 | 67 | M | 1 | Yes | Bitemporal | | | |
| 7 | 20 | M | 2 | Yes | Bitemporal | Bitemporal RNS | | |
| 8 | 30 | M | 4 | Yes | Bitemporal | Palliative right ATL | Hippocampal sclerosis | Seizure-free at 8 months |
| 9 | 67 | F | 3 | No | Left | | | |
| 10 | 42 | F | 3 | Yes | Bitemporal | Palliative left ATL | Hippocampal sclerosis | <3 months follow-up |
| 11 | 39 | F | | | Bitemporal | Palliative right ATL | Hippocampal gliosis | Continued seizures |
| 12 | 41 | M | | | Bitemporal | | | |
| 13 | 57 | M | | | Right | Right ATL | Hippocampal sclerosis | Seizure-free at 5 months |
| 14 | 25 | F | | | Right | Right ATL | Hippocampal sclerosis | Lost to follow-up |
| 15 | 10 | M | | | | | | |
| 16 | 53 | M | | | Bitemporal | | | |
| 17 | 51 | F | | | | | | |
| 18 | 57 | F | | | Bitemporal | Palliative left ATL | Hippocampal sclerosis | Seizure-free at 1 year |
| 19 | 37 | F | | | Bitemporal | Bitemporal RNS | | |
| 20 | 35 | M | | | Bitemporal | | | |
| 21 | 37 | F | | | Bitemporal | Bitemporal RNS | | |
| 22 | 58 | M | | | Left | Left ATL | Hippocampal sclerosis | Seizure-free at 5 months |
| 23 | 24 | F | | | Bitemporal | | | |

ATL = anterior temporal lobectomy; RNS = responsive neural stimulator.

If a seizure's description was ambiguous, seizure videos were reviewed. Fourteen of 25 scalp-negative seizures occurred during sleep, and nine of these 14 were associated with awakening from sleep, while the other five did not show clear clinical changes. Eleven of 25 scalp-negative seizures occurred during wakefulness. Four of these 11 were associated with subtle clinical symptoms. Three seizures came from one patient and were associated with an internal sensation that caused the patient to push the event button, followed by staring and reduced responsiveness. The fourth seizure came from a different patient and was associated with sudden eye opening and nose scratching, from an eyes-closed, awake resting state. Seven of the 11 seizures during wakefulness did not have a clear clinical correlate, though for most, patients were not interacting with anyone at the time of the seizures. Thus, it is possible that these seizures were associated with alterations in mentation that we were unable to detect.

We compared the semiology of scalp-negative seizures to that of scalp-positive seizures for each patient. Nine of 10 patients with scalp-negative seizure records also had scalp-positive seizures. In six of these nine patients, the semiology of scalp-negative seizures was similar to that of scalp-positive seizures, particularly at seizure onset, though scalp-positive seizures often progressed to involve additional symptoms such as oral/manual automatisms and unresponsiveness. Of the remaining three patients, two had scalp-negative seizures that occurred during wakefulness without a clear clinical correlate, whereas their scalp-positive seizures occurred during wakefulness and involved vocalization with reduced responsiveness or oral/manual automatisms. One patient had scalp-negative seizures that occurred during sleep and resulted in awakening, but had scalp-positive seizures that occurred during wakefulness and involved an epigastric sensation, oral/manual automatisms, and unresponsiveness.

## Seizure detection using coherence features

We first built a scalp-negative seizure detector based on scalp EEG coherence features. To reduce this feature set to those features most important for seizure classification, we applied an automated feature selection algorithm that removes features successively, based on the *P*-values of their logistic regression coefficients. We seeded the automated feature selection algorithm with all 1500 scalp EEG coherence features. As shown in Fig. 4A and B, removal of irrelevant coherence features resulted in a substantial improvement in seizure detection rates and reduction in false alarm rates on cross-validation. The best performance was seen with a selection of 191 coherence features. On cross-validation, this detector correctly

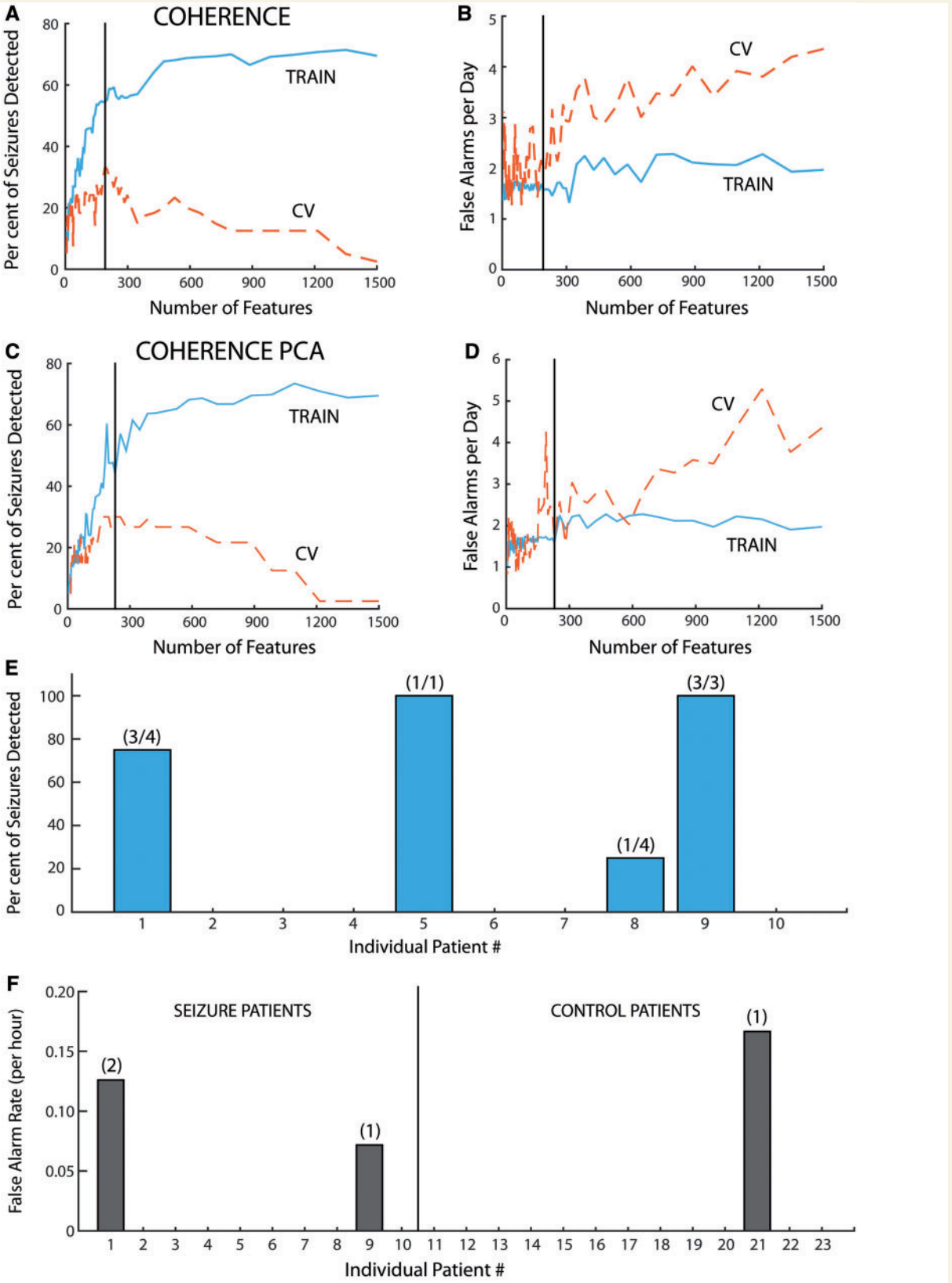


**Figure 4 Scalp-negative seizure detection using coherence features.** (**A** and **B**) Training and cross-validation (CV) performance for automated backwards feature selection of the coherence feature set, including per cent of seizures detected (**A**) and daily false alarm rate (**B**). The solid blue line represents training performance, while the red dashed line represents cross-validation performance. The algorithm starts with all 1500 coherence features (starts at the right side of each graph), and at each iteration, features that have the least predictive value for seizure detection are discarded. As the algorithm progresses, the number of coherence features becomes smaller (we move from the right side of the

(continued)

identified scalp-negative seizures in 50% of patients. Nine of 25 seizures were detected, with an average of 33% of seizures detected per patient. The average cross-validation false alarm rate was 0.082 per hour (~1.97 per day).

We also created a different seizure detector based on PCA of the original coherence features. PCA conserves the information within the original coherence data, but transforms the data to a new coordinate system in which successive orthogonal axes are chosen based on the direction of highest remaining variance in the original dataset. We used the automated feature selection algorithm to narrow the set of 1500 coherence PCA features to those most useful for seizure classification. This approach differs from principal component regression in that we do not assume that the principal components that explain the most variance in the dataset are also the components most useful for classification. Using the automated feature selection algorithm, we reduced the coherence PCA feature set from 1500 features to an optimal selection of 229 features (Fig. 4C and D). On cross-validation, this detector successfully identified scalp-negative seizures in 40% of patients with scalp-negative seizures. Eight of 25 seizures were detected, with an average of ~30% of seizures detected per patient. An average false alarm rate of 0.07 per hour (~1.7 per day) was seen.

Finally, we combined the coherence and the coherence PCA detectors above, with the requirement that in order for a detection to be considered valid, it had to be captured in both detectors. Our reasoning was that both coherence and coherence PCA detectors would be trained to recognize the coherence changes associated with scalp-negative seizures and should thus detect similar seizures. However, because the coherence information is represented on two different coordinate systems and specific features are selected independently for each detector, any noise or false alarms would likely differ between the two detectors.

Combining the coherence and coherence PCA detectors resulted in similar performance with regards to seizure detection, compared to the individual detectors. The combined detector correctly identified scalp-negative seizures in 40% of patients, with an average of 30% of seizures being detected per patient. Eight of 25 seizures were correctly detected (Fig. 4E). All seizure detections were made specifically on the side of seizure onset: all eight left-sided seizures were detected only by the left-sided seizure detectors, whereas one right-sided seizure was detected only by the right-sided detectors. Importantly, combining the coherence and coherence PCA detectors resulted in a marked reduction in false alarms. Only four false alarms from three patients were seen in both detectors (Fig. 4F), translating to an average false alarm rate of 0.0158 per hour (0.38 false alarms per day). Overall, 12 detections were seen with combined coherence and coherence PCA detectors, including eight seizure detections and four false alarms; this yielded a positive predictive value of 67%.

## Example seizure detections and missed detections

Figure 5 shows two examples of seizures that were successfully detected using the combined coherence detectors above. Detected seizure epochs were most often characterized by high amplitude, high frequency ictal activity on the foramen ovale electrodes. Supplementary Fig. 1 shows two examples of scalp-negative seizures, which escaped detection from the combined coherence detectors. In general, these seizures were characterized by being either very focal (involving only one or two foramen ovale electrode contacts) or having lower frequency and often lower amplitude ictal activity on the foramen ovale electrodes.

## Improvement in detector performance after false alarm analysis

Analysis of false alarms can yield important insights into how a detector functions, by revealing common themes that may arise among examples that are challenging for the detector. Analysis of the false alarms raised by the combined coherence and coherence PCA detectors was quite informative. Three of the four false alarms raised by the combined coherence and coherence PCA detectors occurred during sleep-to-wake transitions (Fig. 6). The fourth false alarm was not actually a false alarm, but rather, correct detection of a scalp-negative mesial temporal lobe seizure that had not been reported in the patient's clinical EEG report and had thus escaped our attention. Correcting for this 'false' false alarm, the actual performance of the combined coherence and coherence PCA detector improves: the false alarm rate decreases to 0.013 per hour (0.31 per day), and the positive predictive value increases to 75% (nine seizure detections with three false alarms).

**Figure 4** Continued

graph to the left). Vertical bars indicate the optimal set of features based on cross-validation performance. (**C** and **D**) Similar to **A** and **B**, but for the coherence PCA feature set. (**E** and **F**) Results of combined coherence and coherence PCA detection. (**E**) Bar graph showing the per cent of scalp-negative seizures detected for each of the 10 patients with scalp-negative seizures. Numbers above the bars indicate the number of seizures detected over the total number of seizures for each patient. (**F**) Bar graph showing false alarm rates per hour for all 23 patients. Numbers above the bars indicate the number of false alarms raised for each patient.

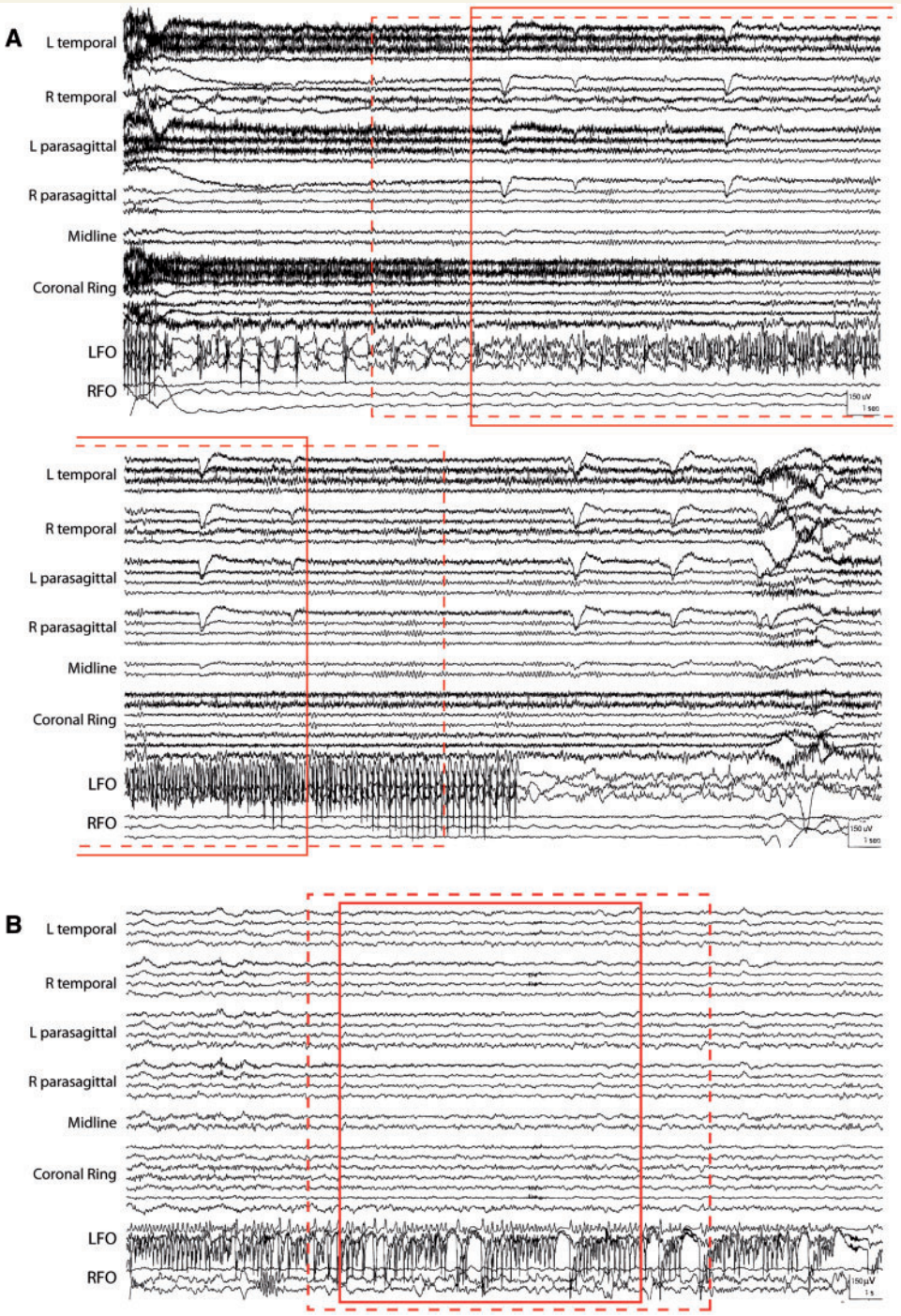


**Figure 5 Examples of scalp-negative seizures that were successfully detected using the combined coherence and coherence PCA detectors.** EEG montages are the same as in Fig. 1. (**A**) Seizure from Patient 1. The two panels represent consecutive pages of EEG recording. The solid red box indicates the epoch detected by the coherence detector, whereas the dashed red box indicates epoch detected by the coherence PCA detector. (**B**) Seizure from Patient 9 that was detected with combined coherence detectors. The solid red box indicates the epoch detected by the coherence detector, whereas the dashed red box indicates epoch detected by the coherence PCA detector.

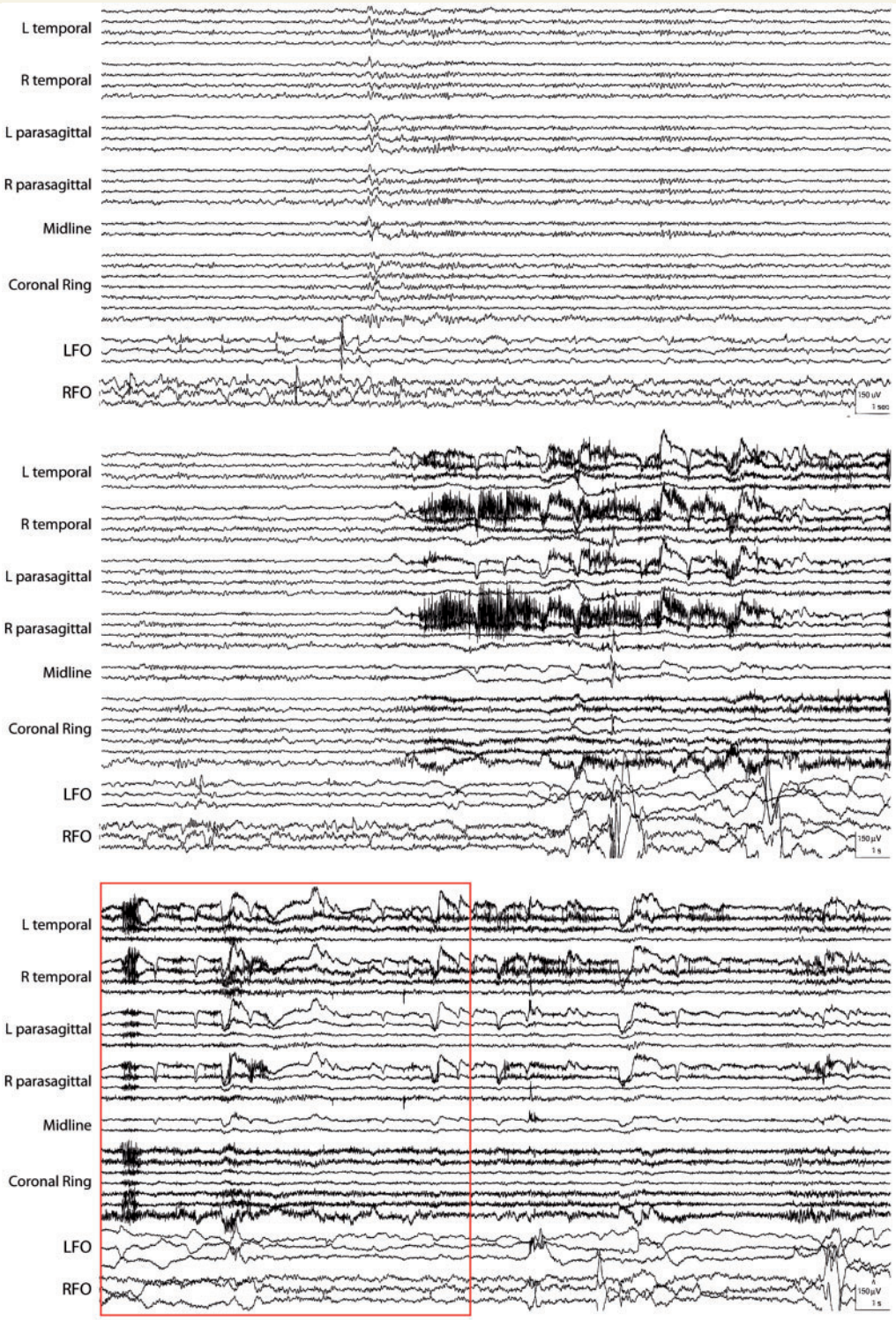


**Figure 6 Example of a typical false alarm from the combined coherence and coherence PCA detectors.** Three consecutive pages of EEG recording are shown. The EEG montage is the same as in Fig. 1. The red box outlines the portion of the EEG that was erroneously detected as a seizure. Note that the false alarm occurs around the time of a sleep-wake transition.

## Detected seizures occur during sleep and are associated with sleep-wake transitions

With three false alarms occurring at the time of sleep-wake transitions, we next questioned whether the detected seizures were also associated with sleep-wake transitions. Based on clinical EEG reports and review of seizure videos when needed, we found that eight of the nine scalp-negative seizures detected occurred during sleep. Six of these eight seizures were associated with clear awakening from sleep (eye opening and movement in bed). Interestingly, the sleep-to-awake transitions occurred around the time when seizures evolved to show higher frequency (15–30 Hz) ictal activity on the foramen ovale electrodes. The remaining two of the eight detected seizures from sleep were not associated with a clear awakening, though both showed an increase in myogenic artefact occurring at the end of or just after the seizures ended on scalp EEG. Thus, our seizure detector primarily recognizes a subset of scalp-negative mesial temporal lobe seizures that occur from sleep and that may be associated with awakening or subtle arousal from sleep.

As an additional *post hoc* control, we tested our seizure detector on scalp-positive seizure records from all six control patients who had scalp-positive seizures. While our detector was trained on scalp-negative seizures, we hypothesized that some scalp-positive seizures might also be detected, particularly if the same mesial temporal lobe structures or networks were activated. For all scalp-positive records (36 h in total), the detector raised one seizure alarm. This was a right-sided detection that corresponded to the onset of a right temporal, scalp-positive seizure. Interestingly, this seizure occurred during sleep and was associated with awakening from sleep. The remaining five scalp-positive seizures, which went undetected, all occurred from the awake state.

# Discussion

A significant fraction of mesial temporal lobe seizures lack a visually identifiable ictal correlate on scalp EEG, and currently, invasive intracranial recordings are the only means by which to identify this activity. The lack of a visible ictal correlate on scalp EEG is often attributed to the deep and focal nature of these seizures. Here, we demonstrate the ability to non-invasively detect a subset of these scalp-negative seizures, using scalp EEG functional connectivity measures. Our scalp-negative mesial temporal lobe seizure detector, which uses scalp EEG coherence features as inputs, correctly identified scalp-negative mesial temporal lobe seizures in 40% of patients. This represents a significant improvement in our ability to non-invasively identify these seizures, given that none of these patients would have previously been identified as having scalp-negative seizures based on routine clinical interpretation of their scalp EEGs. Our seizure detector is patient-independent and can be applied to new patients, without requiring any *a priori* knowledge of their interictal or ictal EEG patterns. Importantly, our results strongly suggest that even the most focal of seizures may involve extensive neural networks.

Optimization of sensitivity and specificity is a trade-off for any detector, and we prioritized minimization of the false alarm rate over sensitivity of detection, to minimize any potential harm to patients. Failing to detect a scalp-negative seizure does not change the current management for most patients, as these seizures currently go undetected (i.e. most patients do not undergo intracranial monitoring needed to detect these seizures). False detection, however, could trigger initiation or intensification of anticonvulsant treatment or lead to invasive investigation with intracranial electrodes, which could cause unnecessary morbidity and cost to the patient. Importantly, our scalp-negative mesial temporal lobe seizure detector has a low false alarm rate of only 0.31 per day, meaning that our detector raises, on average, one false alarm for every 3.2 days of scalp EEG recording. Our detector has a positive predictive value of 75%, meaning that three out of every four alarms raised are true seizure detections. Eighty per cent of the patients in whom seizure alarms were raised actually had scalp-negative seizures, and among the 13 control patients in our dataset (none of whom had scalp-negative seizures), our detector raised a false alarm in only one patient (8%).

An important issue is in how well and to whom the results of our seizure detector generalize. We made several methodological choices to ensure that our results would generalize to the most common clinical settings. First, data from foramen ovale electrodes (rather than depth electrodes) were used, so that our detector could be applied to patients with normal, intact skulls. Second, EEG reviewers analysed the scalp EEG data as they would for clinical purposes, so that our results would generalize to the clinical situation in which scalp-negative seizures are missed on routine visual analysis. Third, we used a standard 10–20 scalp EEG montage with anterior temporal electrodes to review the data and train our detector, so that our results would apply to scalp EEG data collected from most epilepsy monitoring units.

Interestingly, our combined coherence detector appears to recognize a subset of scalp-negative mesial temporal lobe seizures that occur during sleep and that often result in an awakening from sleep. While one concern would be that the detector simply detects sleep-wake transitions rather than scalp-negative seizures, we find this unlikely. First, all seizure detections made were specifically on the side of seizure onset. Second, while a 'normal' sleep-wake transition would be symmetric on scalp EEG, our detector does not detect symmetric changes, as any alarm raised simultaneously on both left- and right-sided detectors is discarded. Last, if the detector was capturing sleep-wake transitions, we would expect a much higher false alarm rate than is seen. It is possible that our scalp-negative

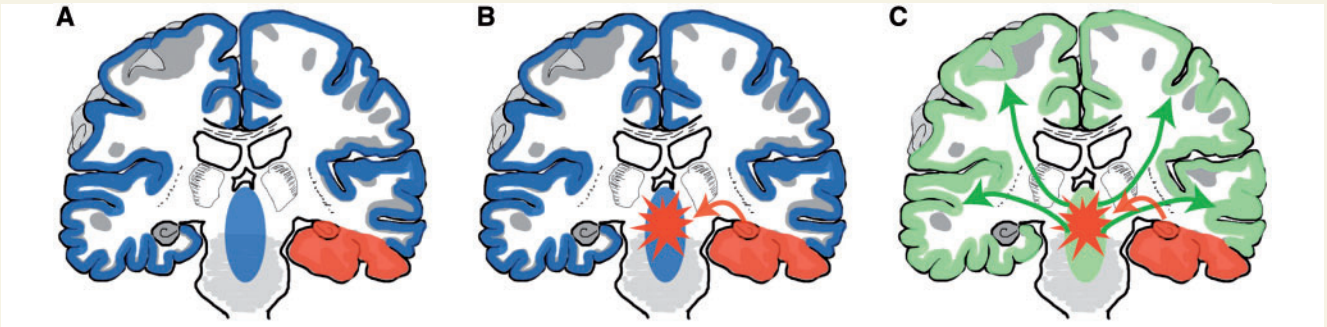


**Figure 7 Ictal activation of arousal networks results in awakening from sleep during scalp-negative mesial temporal lobe seizures.** (**A**) During sleep, subcortical arousal systems are inhibited and cortical activity is reduced. A focal seizure starts in the mesial temporal lobe. (**B**) Spread of seizure to activate the midline subcortical arousal system. (**C**) Ictal activation of arousal systems results in reduction of large amplitude slowing and increase in higher frequency EEG activity, with awakening from sleep.

seizure detector primarily detects seizures that arise during sleep, because these are easier to detect than those that arise during the awake state. In other words, the contrast between non-seizure and seizure states may be greater in the asleep state compared to the awake state, making scalp-negative seizures that occur in sleep more amenable to detection.

An alternative explanation, which also accounts for why many of the detected seizures involve an awakening from sleep, is that our detector recognizes long-range network effects of scalp-negative mesial temporal lobe seizures as they impact the subcortical arousal systems. These scalp-negative seizures start focally in the mesial temporal lobe during sleep, then could either spread to, or indirectly activate midline subcortical arousal systems (e.g. thalamus or midbrain reticular formation), causing a decrease in slowing, an increase in higher frequency EEG activity, and in some cases, an awakening from sleep (Fig. 7). This hypothesis is supported by an increasing body of literature bolstering the concept of focal seizures as a more widespread network phenomenon (Zaveri *et al.*, 2009; Fahoum *et al.*, 2012; Kramer and Cash, 2012; Laufs, 2012). In particular, our hypothesis is complementary to the 'network inhibition hypothesis' put forward by Blumenfeld and colleagues to explain how unilateral temporal lobe seizures during wakefulness might cause a decrease in level of consciousness: here, seizures start focally in the temporal lobe during the awake state and spread to involve the midline arousal systems, where inhibition of these systems results in network inhibition of the bilateral frontoparietal association cortices, causing a 'sleep-like' state (Norden and Blumenfeld, 2002; Blumenfeld, 2012). We posit that a complementary phenomenon occurs during scalp-negative temporal lobe seizures that occur from sleep and that result in arousal from sleep. Interestingly, our detector also raised a seizure alarm for a scalp-positive temporal lobe seizure that occurred from sleep and resulted in an awakening from sleep. Given the similarities in semiology, we hypothesize that similarities in network activation properties also exist between these seizures to account for the detection of this scalp-positive seizure by our scalp-negative seizure detector.

Development of our scalp-negative mesial temporal lobe seizure detector represents a novel and important first step in using computational approaches to non-invasively detect deep seizure activity. While we used scalp EEG coherence features to detect a subset of scalp-negative mesial temporal lobe seizures, our approach can easily be expanded upon to create detectors that recognize other scalp-negative seizure types. Scalp-negative seizures can differ based on the source of ictal activity, the networks activated by this ictal activity, and the sleep-wake states in which these seizures occur. Detectors that are trained to recognize different types of scalp-negative seizures and that use different quantitative scalp EEG features will greatly improve our ability to non-invasively detect (and perhaps even localize) scalp-negative seizure activity.

While the existence of scalp-negative seizures was described decades ago, the clinical significance of these seizures remains largely unknown. Scalp-negative seizures can have subtle clinical manifestations, including brief arousals from sleep and reduced responsiveness in the awake state. Potentially, these seizures might account for some of the sleep disturbances or cognitive complaints often seen in patients with temporal lobe epilepsy. While some scalp-negative seizures do not appear to have any clinical manifestations, it is important to note that direct assessment of mental status was not possible for most of these seizures. Even brief interictal epileptiform discharges from the hippocampus have been shown to have transient adverse effects on cognition when appropriate clinical assessments are made (Kleen *et al.*, 2013), and we hypothesize that most scalp-negative seizures will involve some alteration in mentation when appropriate testing is performed.

While our scalp-negative mesial temporal lobe seizure detector has clear clinical utility in patients with temporal lobe epilepsy, this detector could also be instrumental for studying related neurological disorders, in particular, Alzheimer's disease. Many similarities have been drawn

between temporal lobe epilepsy and Alzheimer's disease (Palop and Mucke, 2009; Noebels, 2011; Scharfman, 2012; Chin and Scharfman, 2013). Patients with Alzheimer's disease have a 6- to 10-fold increased risk of developing epilepsy compared to age-matched controls (Hauser *et al.*, 1986; Hesdorffer *et al.*, 1996), and increasing evidence points to a high prevalence of seizures arising from the temporal lobe (Rao *et al.*, 2009; Vossel *et al.*, 2013; Horvath *et al.*, 2016). Despite the increased risk of seizures, only 2–6% of the routine scalp EEGs in patients with Alzheimer's disease demonstrate epileptiform abnormalities (Liedorp *et al.*, 2010; de Waal *et al.*, 2011; Vossel *et al.*, 2013). It has been hypothesized that scalp-negative mesial temporal lobe epileptiform abnormalities occur frequently in patients with Alzheimer's disease (Noebels, 2011; Horvath *et al.*, 2016), though this possibility has never been tested due to the lack of appropriate tools. Our scalp-negative seizure detector provides a first opportunity to address this hypothesis and may thus provide important insights into the neurophysiology and natural history of epilepsy in relation to Alzheimer's disease.

## Acknowledgements

We thank John Guttag, Brandon Westover, and Siddharth Biswal for useful discussion; Jason Naftulin and Nicole Rivilis for technical support; and the Enterprise Research Infrastructure & Services at Partners Healthcare for the provision and maintenance of the High Performance Computing environment and the Linux computing clusters on which much of our data analysis was performed.

## Funding

A.D.L. was supported by NIH-NINDS R25-NS065743. S.S.C. was supported by NIH-NINDS R01-NS062092 and K24-NS088568.

## Supplementary material

Supplementary material is available at *Brain* online.

## References

Bartolomei F, Wendling F, Vignal JP, Kochen S, Bellanger JJ, Badier JM, et al. Seizures of temporal lobe epilepsy: identification of subtypes by coherence analysis using stereo-electro-encephalography. Clin Neurophysiol 1999; 110: 1741–54.

Blumenfeld H. Impaired consciousness in epilepsy. Lancet Neurol 2012; 11: 814–26.

Chin J, Scharfman HE. Shared cognitive and behavioral impairments in epilepsy and Alzheimer's disease and potential underlying mechanisms. Epilepsy Behav 2013; 26: 343–51.

de Waal H, Stam CJ, Blankenstein MA, Pijnenburg YA, Scheltens P, van der Flier WM. EEG abnormalities in early and late onset Alzheimer's disease: understanding heterogeneity. J Neurol Neurosurg Psychiatry 2011; 82: 67–71.

Delorme A, Makeig S. EEGLAB: an open source toolbox for analysis of single-trial EEG dynamics including independent component analysis. J Neurosci Methods 2004; 134: 9–21.

Ebersole JS, Pacia SV. Localization of temporal lobe foci by ictal EEG patterns. Epilepsia 1996; 37: 386–99.

Engel J Jr. Mesial temporal lobe epilepsy: what have we learned? Neuroscientist 2001; 7: 340–52.

Fahoum F, Lopes R, Pittau F, Dubeau F, Gotman J. Widespread epileptic networks in focal epilepsies: EEG-fMRI study. Epilepsia 2012; 53: 1618–27.

Hauser WA, Morris ML, Heston LL, Anderson VE. Seizures and myoclonus in patients with Alzheimer's disease. Neurology 1986; 36: 1226–30.

Hesdorffer DC, Hauser WA, Annegers JF, Kokmen E, Rocca WA. Dementia and adult-onset unprovoked seizures. Neurology 1996; 46: 727–30.

Horvath A, Szucs A, Barcs G, Noebels JL, Kamondi A. Epileptic Seizures in Alzheimer Disease: a review. Alzheimer Disease Assoc Disord 2016; 30: 186–92.

Kleen JK, Scott RC, Holmes GL, Roberts DW, Rundle MM, Testorf M, et al. Hippocampal interictal epileptiform activity disrupts cognition in humans. Neurology 2013; 81: 18–24.

Kramer MA, Cash SS. Epilepsy as a disorder of cortical network organization. Neuroscientist 2012; 18: 360–72.

Laufs H. Functional imaging of seizures and epilepsy: evolution from zones to networks. Curr Opin Neurol 2012; 25: 194–200.

Lieb JP, Walsh GO, Babb TL, Walter RD, Crandall PH. A comparison of EEG seizure patterns recorded with surface and depth electrodes in patients with temporal lobe epilepsy. Epilepsia 1976; 17: 137–60.

Liedorp M, Stam CJ, van der Flier WM, Pijnenburg YA, Scheltens P. Prevalence and clinical significance of epileptiform EEG discharges in a large memory clinic cohort. Dement Geriatr Cogn Disord 2010; 29: 432–7.

Mitra P, Bokil H. Observed brain dynamics. New York, NY: Oxford University Press; 2008.

Noebels J. A perfect storm: converging paths of epilepsy and Alzheimer's dementia intersect in the hippocampal formation. Epilepsia 2011; 52 (Suppl 1): 39–46.

Norden AD, Blumenfeld H. The role of subcortical structures in human epilepsy. Epilepsy Behav 2002; 3: 219–31.

Pacia SV, Ebersole JS. Intracranial EEG substrates of scalp ictal patterns from temporal lobe foci. Epilepsia 1997; 38: 642–54.

Palop JJ, Mucke L. Epilepsy and cognitive impairments in Alzheimer disease. Arch Neurol 2009; 66: 435–40.

Rao SC, Dove G, Cascino GD, Petersen RC. Recurrent seizures in patients with dementia: frequency, seizure types, and treatment outcome. Epilepsy Behav 2009; 14: 118–20.

Sanchez PE, Zhu L, Verret L, Vossel KA, Orr AG, Cirrito JR, et al. Levetiracetam suppresses neuronal network dysfunction and reverses synaptic and cognitive deficits in an Alzheimer's disease model. Proc Natl Acad Sci USA 2012; 109: E2895–903.

Scharfman HE. Alzheimer's disease and epilepsy: insight from animal models. Future Neurol 2012; 7: 177–92.

Sheth SA, Aronson JP, Shafi MM, Phillips HW, Velez-Ruiz N, Walcott BP, et al. Utility of foramen ovale electrodes in mesial temporal lobe epilepsy. Epilepsia 2014; 55: 713–24.

Vossel KA, Beagle AJ, Rabinovici GD, Shu H, Lee SE, Naasan G, et al. Seizures and epileptiform activity in the early stages of Alzheimer disease. JAMA Neurol 2013; 70: 1158–66.

Wennberg R, Arruda F, Quesney LF, Olivier A. Preeminence of extrahippocampal structures in the generation of mesial temporal seizures: evidence from human depth electrode recordings. Epilepsia 2002; 43: 716–26.

Wieser HG, Elger CE, Stodieck SR. The 'foramen ovale electrode': a new recording method for the preoperative evaluation of patients suffering from mesio-basal temporal lobe epilepsy. Electroencephalogr Clin Neurophysiol 1985; 61: 314–22.

Zaveri HP, Duckrow RB, de Lanerolle NC, Spencer SS. Distinguishing subtypes of temporal lobe epilepsy with background hippocampal activity. Epilepsia 2001; 42: 725–30.

Zaveri HP, Pincus SM, Goncharova, II, Duckrow RB, Spencer DD, Spencer SS. Localization-related epilepsy exhibits significant connectivity away from the seizure-onset area. Neuroreport 2009; 20: 891–5.